Polymer 51 (2010) 5869–5882

Contents lists available at ScienceDirect

Polymer

journal homepage: www.elsevier.com/locate/polymer

Structure and particle aggregation in block copolymer-binary nanoparticle composites

Houyang Chen*, Eli Ruckenstein**

Department of Chemical and Biological Engineering, State University of New York at Buffalo, Buffalo, NY 14260-4200, USA

ARTICLE INFO

Article history:
Received 18 August 2010
Received in revised form
4 October 2010
Accepted 6 October 2010
Available online 15 October 2010

Keywords:
Dissipative particle dynamics
Block copolymer-particle composites
Aggregates

ABSTRACT

The aggregation behavior and location of binary nanoparticles in a block copolymer-nanoparticle composite are investigated by employing three-dimensional dissipative particle dynamics (DPD) simulations. The dependence of the morphology of the composites and of the composition of the nanoparticle aggregates on the pair interactions between the same and different kinds of nanoparticles or segments, as well as between each kind of nanoparticles and each kind of segments of the block copolymer, is examined. The natures of the two kinds of nanoparticles employed constitute an important factor in the phase behavior of these composites. When the change of the state of some particles from individually distributed to aggregated is induced particularly by the interactions between particles, the configuration of the block copolymer is changed from lamellar to a complex one. In contrast, when the above change in the configuration of the particles (aggregated or nonaggregated) is induced particularly by the interactions between the particles and the segments of the block copolymer, the configuration of the block copolymer remains lamellar. DPD simulations imply repulsive pair interactions between all pairs of particles, segments and particles, as well as segments of the block copolymers. The aggregation observed in simulations, is caused by the collective behavior of the system which transforms the pair repulsive interactions (which are the only ones that are considered in DPD) in a collective attraction.

1. Introduction

Nanocomposites containing both nanoparticles and block copolymers are useful not only because the nanoparticles can enhance the mechanical and optical properties of the materials but also because the block copolymers can affect the organization of nanoparticles. Numerous papers have paid attention to these issues [1–19]. Most of them are focused on one kind of nanoparticles [1–18], and only few consider mixtures of two kinds of nanoparticles [19]. Bockstaller et al. [19], who examined experimentally composites containing a block copolymer (poly(styrene-*b*-ethylene propylene)) and two kinds of nanoparticles, namely gold and silica particles, noted that the morphology of the composites depends on the sizes of the nanoparticle, and that the gold nanocrystals prefer to be located at the interface between the domains generated by polystyrene and poly (ethylene propylene), whereas the large silica nanocrystals are mostly located on the domains generated by poly(ethylene propylene).

By controlling the aggregation of a binary mixture of nanoparticles in nanoparticle-block copolymer composites, one can affect the properties of the composites. In a previous paper, we investigated using DPD simulations the effect of aggregation of a single kind of nanoparticles on the morphology of the block copolymer-nanoparticle composites [18]. In the present paper, the aggregation and locations of a binary mixture of nanoparticles are examined using the same kind of simulations. DPD simulations were successfully employed to examine the phase behavior of block copolymer melts [20–25], as well as the phase behavior of composites containing particles and block copolymers [18]. Following the introduction, the technique of the dissipative particle dynamics simulation is presented in some details in Section 2. In Section 3, various conditions, which affect the aggregation behavior and the location of the nanoparticles in a composite containing a block copolymer and two kinds of nanoparticles, are examined. The conclusions are summarized in the last section.

2. Mesoscale simulation details

2.1. Dissipative particle dynamics method

The dissipative particle dynamics (DPD) simulation was developed [26] by Hoogerbrugge and Koelman in 1992. In DPD simulations, the force that acts on a particle i is composed of three

* Corresponding author.
** Corresponding author. Tel.: +1 716 645 1179; fax: +1 716 645 3822.
E-mail addresses: houyangchen2008@hotmail.com (H. Chen), feaeliru@buffalo.edu (E. Ruckenstein).

0032-3861/$ – see front matter © 2010 Elsevier Ltd. All rights reserved.
doi:10.1016/j.polymer.2010.10.011

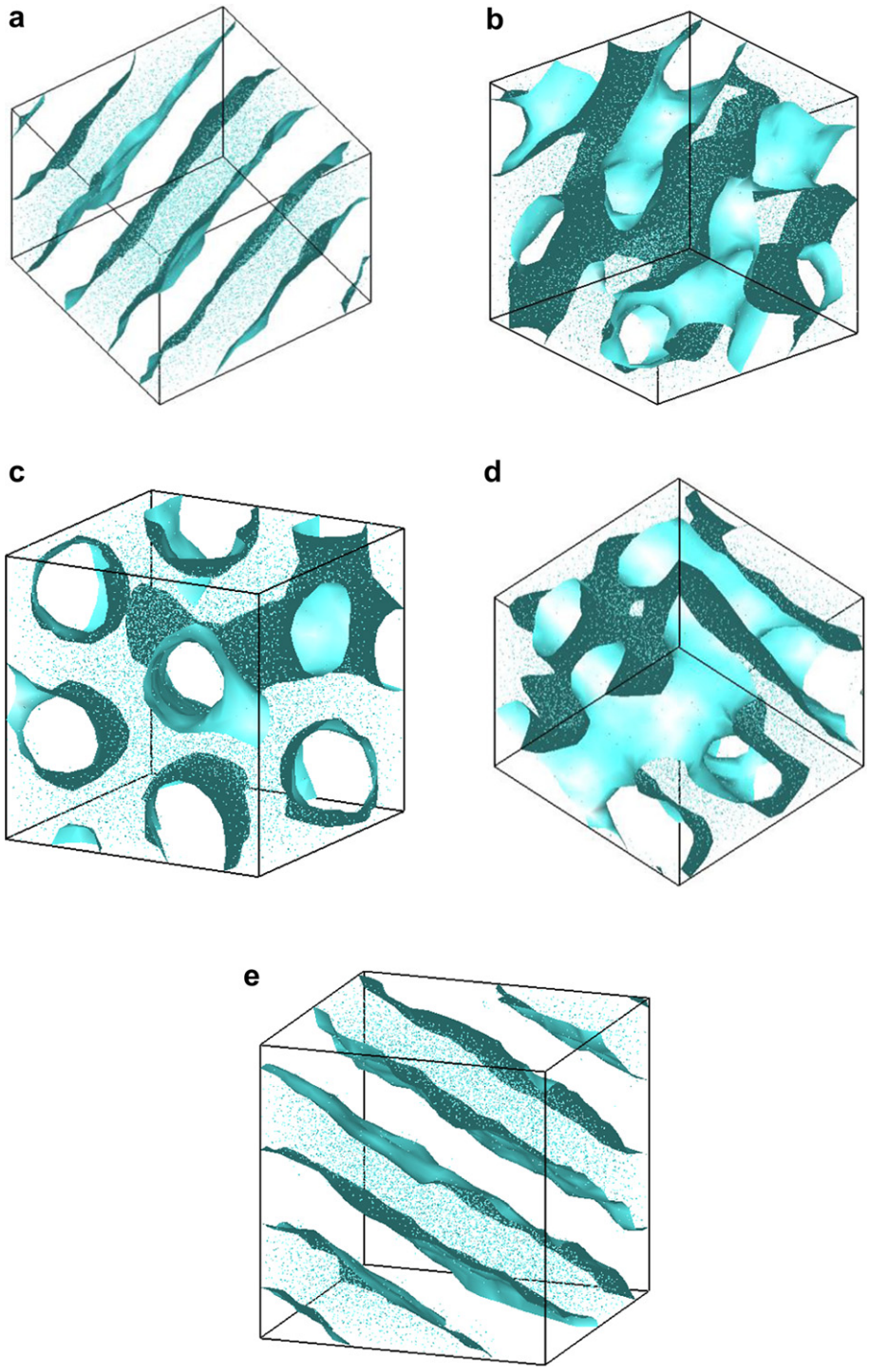

Fig. 1. Phase behavior of pure block copolymer for $a^{*}_{ij} = a_{ij} - 1/2(a_{ii} + a_{jj}) = 15$. (a) $a_{AA} = 25$, $a_{BB} = 25$, $a_{AB} = 40$; (b) $a_{AA} = 15$, $a_{BB} = 35$, $a_{AB} = 40$; (c) $a_{AA} = 15$, $a_{BB} = 75$, $a_{AB} = 60$; (d) $a_{AA} = 25$, $a_{BB} = 65$, $a_{AB} = 60$; (e) $a_{AA} = 45$, $a_{BB} = 45$, $a_{AB} = 60$. A segments: White; B segments: Bluish green. (For interpretation of the references to colour in this figure legend, the reader is referred to the web version of this article).

components: the conservative force $\mathbf{F}^{C}_{ij}$, the dissipative force $\mathbf{F}^{D}_{ij}$, and the random force $\mathbf{F}^{R}_{ij}$, all caused by a j particle.

$$\mathbf{f}_i = \sum_{j \neq i} \left(\mathbf{F}^{C}_{ij} + \mathbf{F}^{D}_{ij} + \mathbf{F}^{R}_{ij} \right) \tag{1}$$

where

$$\mathbf{F}^{C}_{ij} = \begin{cases} a_{ij}(1 - r_{ij}/r_c)\hat{\mathbf{r}}_{ij} & r_{ij} < r_c \\ 0 & r_{ij} \geq r_c \end{cases} \tag{2}$$

$$\mathbf{F}^{D}_{ij} = -\gamma \omega^{D}(r_{ij}) \left(\hat{\mathbf{r}}_{ij} \cdot \mathbf{v}_{ij} \right) \hat{\mathbf{r}}_{ij} \tag{3}$$

$$\mathbf{F}^{R}_{ij} = \sigma \omega^{R}(r_{ij}) \zeta_{ij} \Delta t^{-1/2} \hat{\mathbf{r}}_{ij} \tag{4}$$

a_{ij} being the maximum repulsion between i and j particles, $\mathbf{r}_{ij} = \mathbf{r}_i - \mathbf{r}_j$, $r_{ij} = |\mathbf{r}_{ij}|$, $\hat{\mathbf{r}}_{ij} = \mathbf{r}_{ij}/|\mathbf{r}_{ij}|$, $\mathbf{v}_{ij} = \mathbf{v}_i - \mathbf{v}_j$, $\mathbf{r}_i$ and $\mathbf{v}_i$ are the position and velocity of the i bead, respectively, r_c is the cutoff radius, ω^{D} and ω^{R} are weight contribuions, γ is the friction coefficient, σ is the noise amplitude, Δt is the time step, and ζ_{ij} is

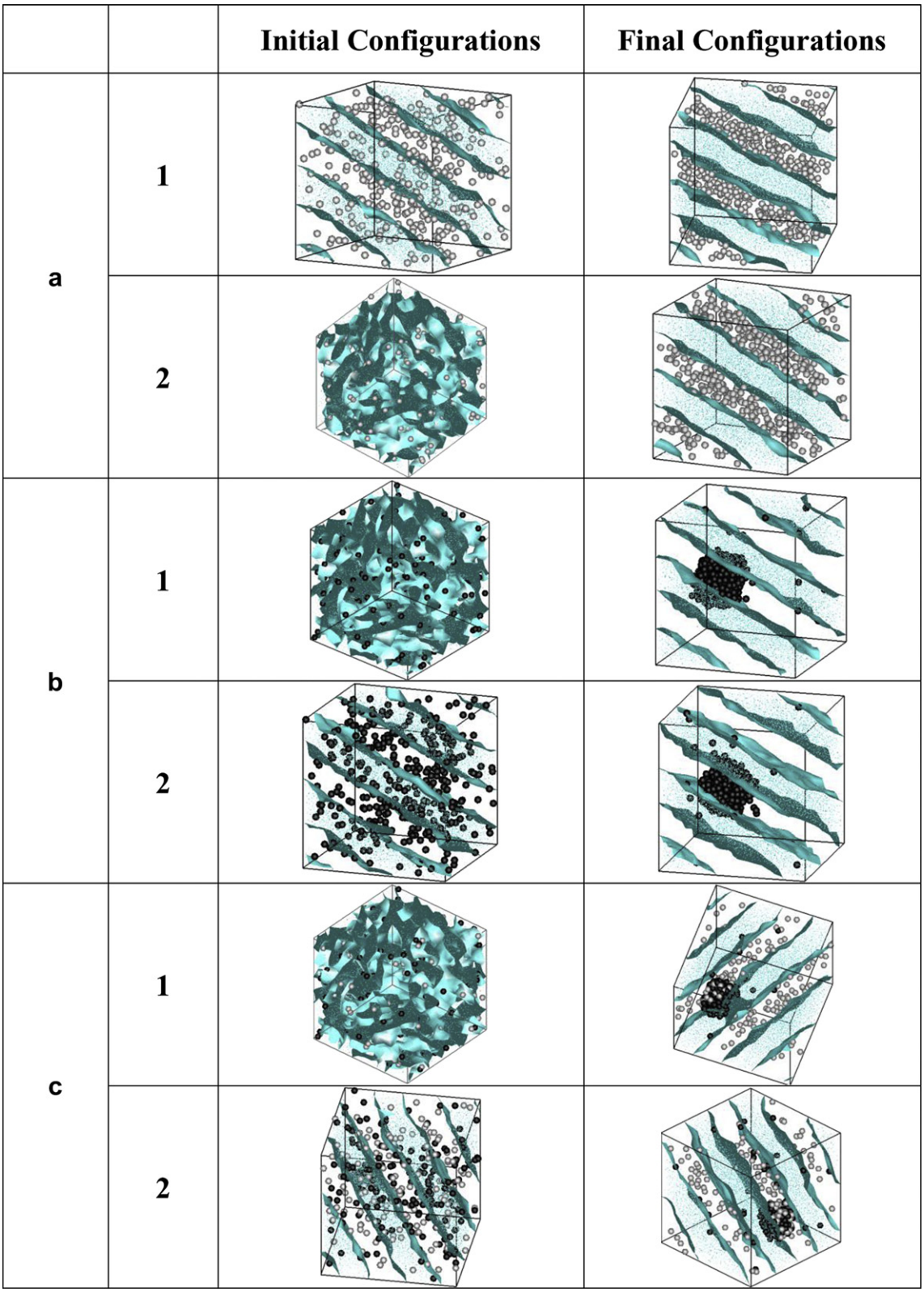

Fig. 2. Initial and final configurations of nanoparticles-block copolymer composites for $a_{AA} = a_{BB} = 25$, $a_{AB} = 40$, $a_{P1P1} = 45$, $a_{P1B} = a_{P2B} = 80$. (a) only P_1 particles, and $a_{P1A} = 30$; (b) only P_2 particles, and $a_{P2P2} = 80$, $a_{P2A} = 90$; (c)binary mixture of P_1 and P_2 nanoparticles, and $a_{P1A} = 30$, $a_{P2P2} = 80$, $a_{P1P2} = 30$, $a_{P2A} = 90$. P_1: Grey; P_2: Black; A segments: White; B segments: Bluish green. The Figures show that different initial configuration with the same DPD parameters result in the final equilibrium results. (For interpretation of the references to colour in this figure legend, the reader is referred to the web version of this article).

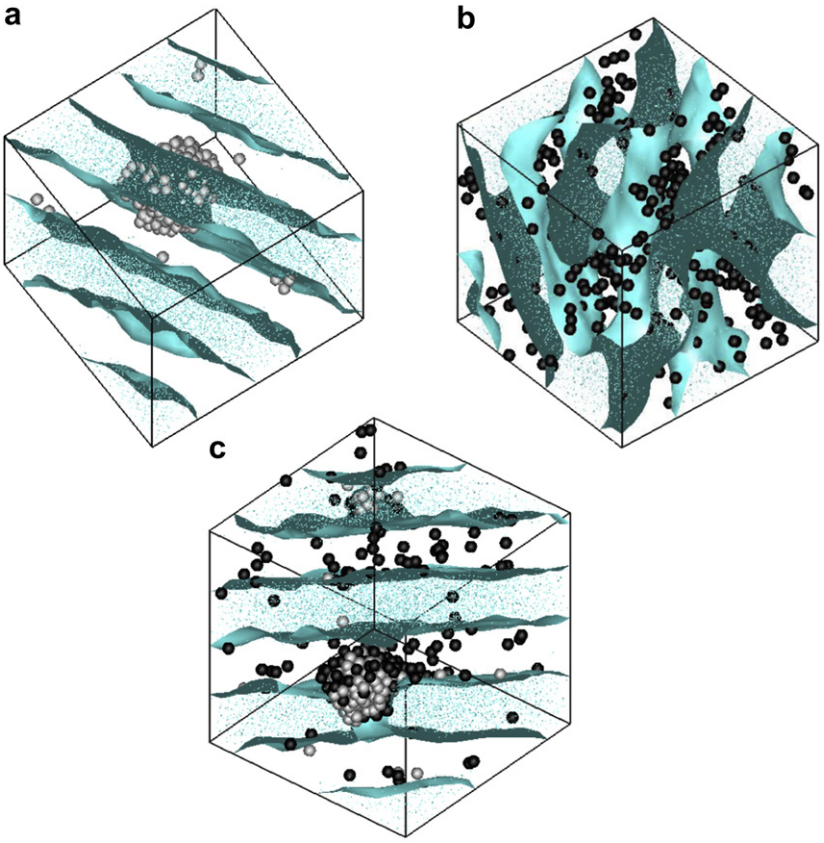

Fig. 3. Phase behavior of nanoparticles-block copolymer composites for $a_{AA} = a_{BB} = 25$, $a_{AB} = 40$. (a) only P_1 particles, and $a_{P1A} = 70$, $a_{P1P1} = 45$, $a_{P1B} = 80$; (b) only P_2 particles, and $a_{P2P2} = 80$, $a_{P2A} = 50$, $a_{P2B} = 80$; (c) Binary mixture of P_1 and P_2 particles, and $a_{P1A} = 70$, $a_{P2P2} = 80$, $a_{P1P2} = 70$, $a_{P2A} = 50$, $a_{P1P1} = 45$, $a_{P1B} = a_{P2B} = 80$. P_1: Grey; P_2: Black; A segments: White; B segments: Bluish green. (For interpretation of the references to colour in this figure legend, the reader is referred to the web version of this article).

a random number with zero mean and *unit* variance. Following Ref. [20],

$$\omega^{D}(r) = \left[\omega^{R}(r)\right]^2 = \begin{cases} (1-r)^2 & r < r_c \\ 0 & r \geq r_c \end{cases} \quad (5)$$

$$\sigma^2 = 2\gamma k_B T \quad (6)$$

where k_B is the Boltzmann constant, and T is the absolute temperature. For a polymer chain, there is an additional bonding force

$$\mathbf{F}_{ij}^{S} = -C\mathbf{r}_{ij} \quad (7)$$

where C is a constant.

The motion is governed by the Newton equation, and the integration of the equations of motion is carried out by using a modified velocity-Verlet algorithm [27] with $\lambda = 0.65$ and a time step $\Delta t = 0.04\tau$, where $\tau = (mr_c^2/k_BT)^{1/2}$[24], m being the mass of a particle or a segment (which are assumed to be the same). The choice of the total number of DPD steps depends on the system. In our paper, most systems reached equilibrium after about 250 000 steps, and some of them reached equilibrium after about 350 000 steps, so we select 600 000 steps. At 800 000 steps, the results coincided with those for 600 000 steps.

2.2. Simulation parameters

In this paper, a composite containing the block copolymer A_5B_5 and two kinds of nanoparticles, P_1 and P_2, is considered. The P_1 and P_2 particles and the A and B segments of the block copolymer are considered as DPD particles with the same size. The simulations were performed in an NVT canonical box of size $(20r_c)^3$. For all three dimensions periodic boundary conditions were used. The number densities of all segments or particles in the volume r_c^3 are 3, and the volume percent of each of the two kinds of nanoparticles is 0.75%. For comparison purposes, in Figs. 2 and 3, we consider systems containing either 1.5% volume pure P_1 or pure P_2 particles in nanoparticle-block copolymer composites. The cutoff radius r_c, the particle mass m, and k_BT were considered as the units. The values of σ and C were taken 3 and 4, respectively [27]. To examine the effect of the nature of particles on the structure of a composites containing a block copolymer and a binary mixture of particles, the parameters a_{P1P2}, a_{P1A}, a_{P2A}, and a_{P2P2} were varied. For the other constant parameters, the following fixed values were used: $a_{AA} = a_{BB} = 25$, $a_{AB} = 40$, $a_{P1P1} = 45$, $a_{P1B} = a_{P2B} = 80$.

For a composite that contains two kinds of particles and a block copolymer (A_5B_5) formed of two kinds of segments, the DPD simulations involve 10 parameters a_{ij}. It is natural to try to reduce the number of parameters by combining some of them. One of the reviewers suggested that because equilibrium is achieved, the three interaction parameters a_{ii}, a_{jj}, and a_{ij} can be reduced to a single effective interaction $a_{ij}^{*} = a_{ij} - 1/2(a_{ii} + a_{jj})$. Obviously, one can thus reduce the number of parameters involved. To verify if such

Table 1
Parameters of pure block copolymer for $a_{ij}^{*} = a_{ij} - 1/2(a_{ii} + a_{jj}) = 15$.

	a_{AB}^{*}	a_{AA}	a_{BB}	a_{AB}
(a)	15	25	25	40
(b)	15	15	35	40
(c)	15	15	75	60
(d)	15	25	65	60
(e)	15	45	45	60

a reduction in the number of parameters is possible, we carried out simulations for the block copolymer A_5B_5 alone. For a selected value of a^*_{ij}, there are various configurations, each dependent on the values of a_{ij}, a_{ii}, and a_{jj}. Hence, a^*_{ij} cannot be associated with a single configuration. Indeed, we present in Table 1 and Fig. 1 various choices for a_{AA}, a_{BB}, and a_{AB} for $a^*_{AB} = 15$ and the morphologies obtained. Because the morphologies are different, it is clear that the effective parameter method is not suitable to be used to reduce the number of parameters. Another possibility is to assume that $a_{ij} = 1/2(a_{ii} + a_{jj})$ or that $a_{ij} = (a_{ii}a_{jj})^{1/2}$. The use of the arithmetic or the geometric mean for a_{ij} reduces the number of parameters, and is now under investigation.

Let us first demonstrate that the results of our simulations are independent of their initial states. Fig. 2 presents three cases, each of them having two different initial configurations. Because the simulation results are the same, it is clear that they are independent of their initial states.

3. Results and discussions

3.1. Comparison between composites containing a block copolymer and either particles P_1, or particles P_2, or a binary mixture of both P_1 and P_2

In Fig. 2a (in the final configurations), for P_1 particles-block copolymer composites, the P_1 particles are located individually or as small aggregates in the domains generated by the A segment of the block copolymer (we call them A domains), whereas for the P_2 particles-block copolymer composites (Fig. 2b), mostly aggregates are generated which are located in the B domains. However, for binary particles-block copolymer composites (Fig. 2c), most of the P_1 particles are located individually in the A domains, and a large aggregate containing both P_1 and mostly P_2 particles is generated. In Fig. 3, some interaction parameters, namely, a_{P1P2}, a_{P1A}, a_{P2A}, are changed compared to Fig. 2.The change in these interactions has substantial effects on the phase behavior. Indeed, this time the P_1 particles of the P1 particle-block copolymer composites form a large aggregate (Fig. 3a), the P_2 particles of the P_2 particles-block copolymer composites are distributed individually or as small aggregates in a complex structure formed by the block copolymer (Fig. 3b). A large aggregate containing both P_1 and P_2 particles as well as particles individually distributed mostly of P_2 (Fig. 3c) are formed in composites containing the block copolymer and the particles P_1 and P_2. Figs. 2 and 3 also show that by replacing a fraction of nanoparticles in single nanoparticles-block copolymer composites with another kind of nanoparticles, one can change the structure of the composite and thus affect its properties.

Aggregates are generated as a result of the cooperative effects of the following interactions: interactions between the particles and the segments of the block copolymer, interactions between the same kinds of particles, as well as interactions between different kinds of particles, and the interactions between segments. However, in the present kind of simulations, one considers that all pair interactions are repulsive. Even though, all pair interactions are repulsive, aggregates, which are located in the A or B domains or at their interface, are formed. This can be explained as follows. Let us consider a group of particles with pair repulsive interactions between them and let select a pair of neighboring particles. Each of

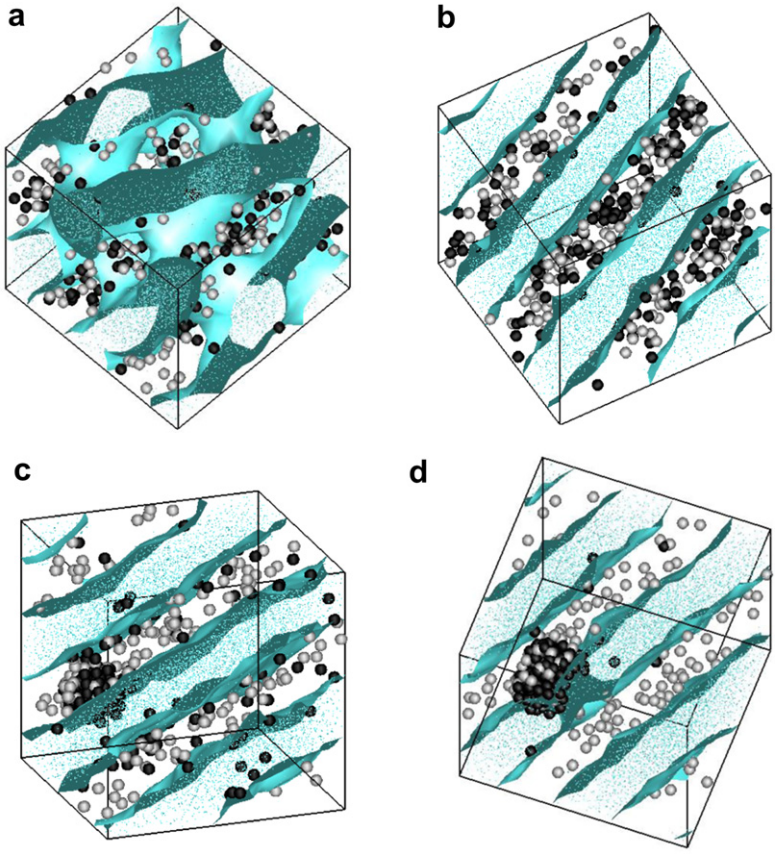

Fig. 4. Phase behavior of a binary mixture of nanoparticles-block copolymer composites as a function of the pair repulsive interaction a_{P2A} between P_2 nanoparticles and A segments of the block copolymer A_5B_5 for $a_{P1A} = 30$, $a_{P2P2} = 80$, $a_{P1P2} = 30$. (a) $a_{P2A} = 30, 40$; (b) $a_{P2A} = 50, 60$; (c) $a_{P2A} = 70, 80$; (d) $a_{P2A} = 90$. P_1: Grey; P_2: Black; A segments: White; B segments: Bluish green. (For interpretation of the references to colour in this figure legend, the reader is referred to the web version of this article).

the particles of this pair is subjected to the repulsion caused by the particles of the group. If this collective repulsion is larger than that between the selected pair, the distance between the two particles of the pair will decrease. In other words, the collective pair repulsion can generate attraction between two repulsive particles.

3.2. Phase behavior of a binary mixture of nanoparticles-block copolymer composites for weak a_{P1P2} interactions

Fig. 4 presents the phase behavior of a binary mixture of nanoparticles-block copolymer composites as a function of a_{P2A} between the P_2 nanoparticles and the A segments of the block copolymer A_5B_5 for $a_{P1A} = 30$, $a_{P2P2} = 80$, $a_{P1P2} = 30$, $a_{AB} = 40$. For a weak repulsion a_{P2A} (e.g. $a_{P2A} = 30$, or 40), a complex structure of the block copolymer is formed (Fig. 4a), and the two kinds of particles P_1 and P_2 are distributed individually or as small aggregates in the A domains. As a_{P2A} between the P_2 nanoparticles and the A segments of the block copolymer increases to 50 or 60, lamellar structures are generated by the block copolymers (Fig. 4b). Both P_1 and P_2 particles are still distributed mostly individually in the A domain, and some small clusters are formed from P_2 particles. If a_{P2A} is varied from 70 to 90, the P_2 particles become incompatible with both A and B segments, and form aggregates located at the interface between the A and B domains, and single P_1 particles or small clusters of P_1 particles are located in the A domains (Fig. 4c and d). Because of the compatibility between P_1 and P_2 particles, some P_1 particles are included in the P_2 aggregates.

In Figs. 4 and 5, a_{P2A} is changed between 30 and 90; in Fig. 4, $a_{P1A} = 30$ whereas in Fig. 5 it is 70. The other parameters are the same in both Figures. Fig. 5 shows that P_1 aggregates are formed when a_{P2A} is changed from 30 to 90. As a_{P2A} increases, the P_2 particles are first distributed mostly individually or as small aggregates (Fig. 5a), then they form small clusters or aggregate together with the P_1 particles (Fig. 5b), and finally, both P_1 and P_2 aggregate together, forming large aggregates (Fig. 5c). Fig. 5 shows that, as a_{P2A} changes from 30 to 90, the location of the P_2 nanoparticles increasingly changes from the A to the B domains.

The phase behavior of a binary mixture of nanoparticles-block copolymer composites as a function of a_{P2P2} for $a_{P1A} = 30$, $a_{P2A} = 60$, $a_{P1P2} = 30$, $a_{AB} = 40$ is presented in Fig. 6. This figure shows that the P_1 particles are individually or as small clusters located in the A domains, whereas the P_2 particles are located as aggregates at the interface between the A and B domains (Fig. 6a). As the repulsive pair interaction between the P_2 particles further increases, the morphology of the block copolymers first acquires a complex structure containing single particles and aggregates (Fig. 6b), then, the aggregates split into single particles and small clusters (Fig. 6c). Further, lamellae are generated from the block copolymer segments (Fig. 6d). The location of the two kind of particles was also examined in papers [28].

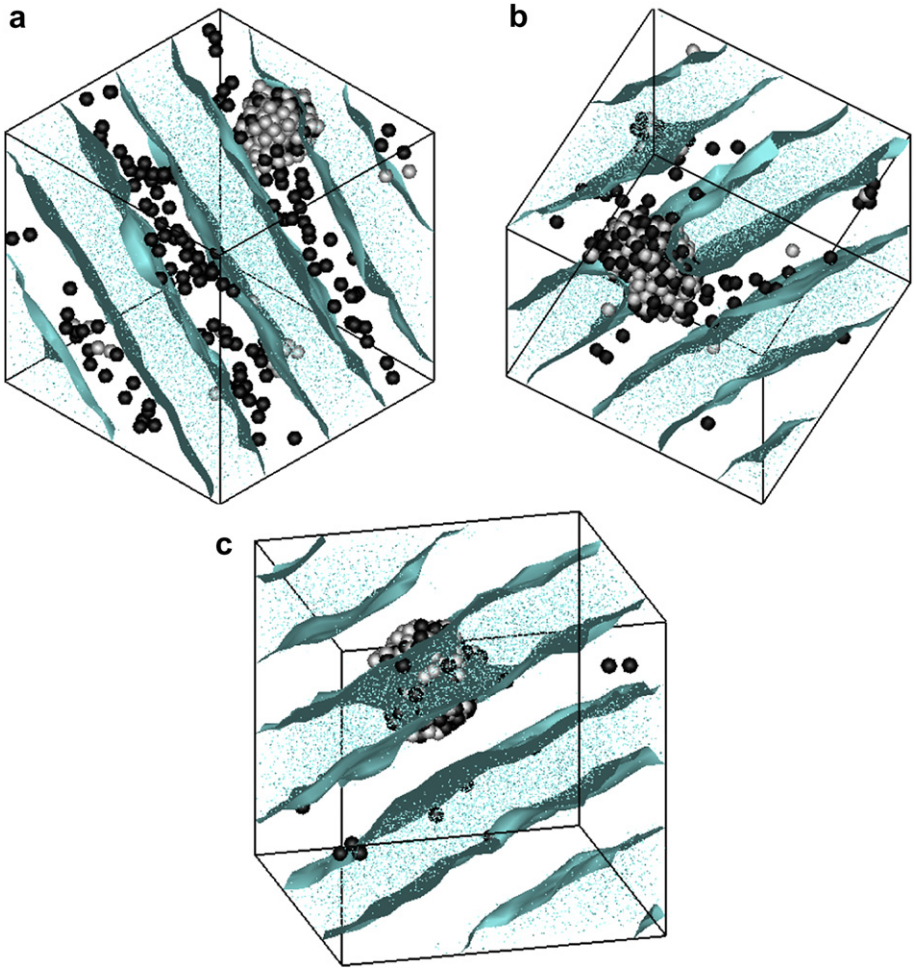

Fig. 5. Phase behavior of a binary mixture of nanoparticles-block copolymer composites as a function of the pair repulsive interaction a_{P2A} between P_2 nanoparticles and A segments of the block copolymer A_5B_5 for $a_{P1A} = 70$, $a_{P2P2} = 80$, $a_{P1P2} = 30$. (a) $a_{P2A} = 30$, 40; (b) $a_{P2A} = 50$, 60; (c) $a_{P2A} = 70$, 80, 90. P_1: Grey; P_2: Black; A segments: White; B segments: Bluish green. (For interpretation of the references to colour in this figure legend, the reader is referred to the web version of this article).

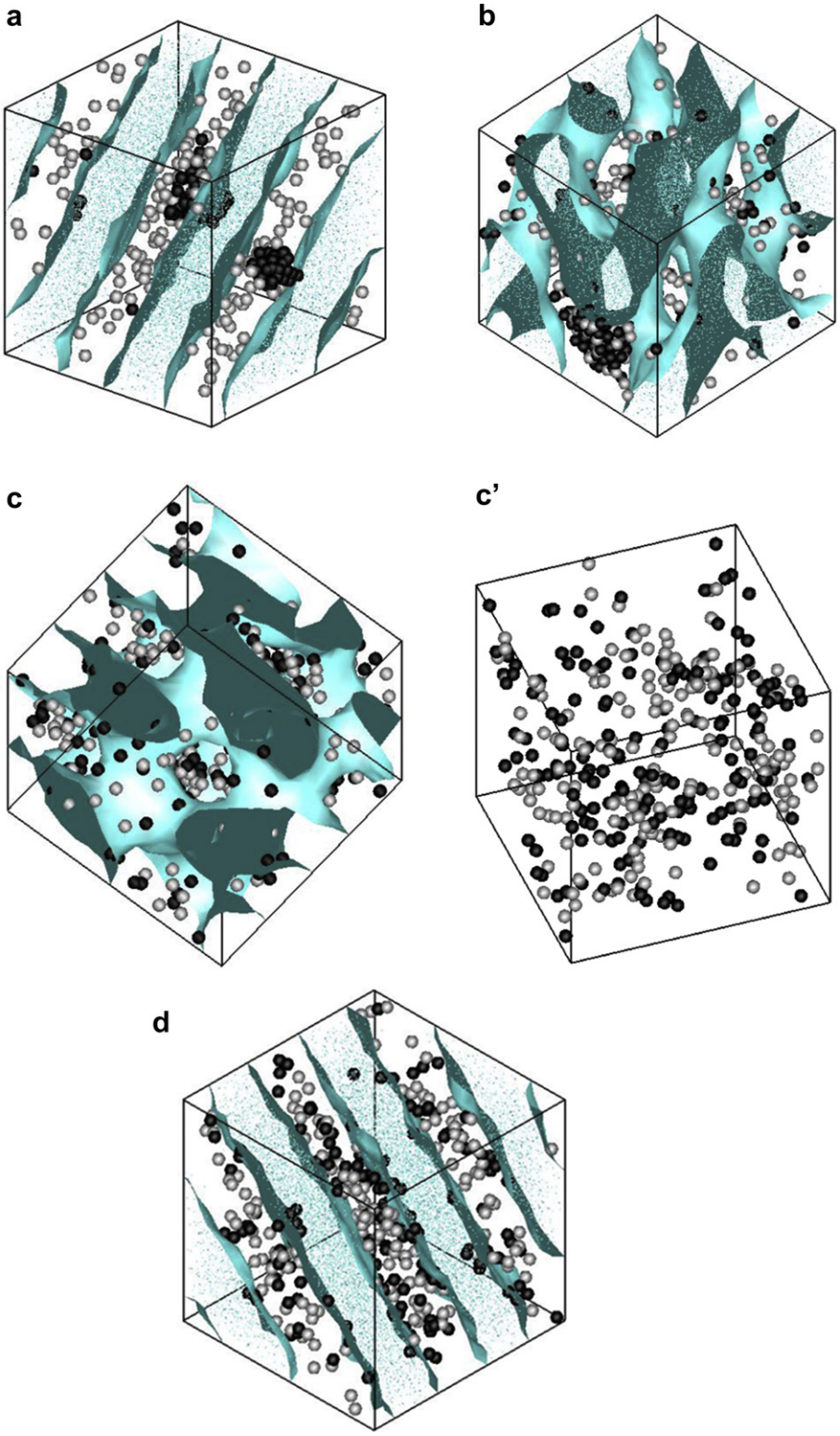

Fig. 6. Phase behavior of a binary mixture of nanoparticles-block copolymer composites as a function of the pair repulsive interaction a_{P2P2} between P_2 nanoparticles for $a_{P1A} = 30$, $a_{P2A} = 60$, $a_{P1P2} = 30$. (a) $a_{P2P2} = 30$, 40,50; (b) $a_{P2P2} = 60$; (c) $a_{P2P2} = 70$; (d) $a_{P2P2} = 80$. In Figures (c′), only the particles of Figures (c) are present. P_1: Grey; P_2: Black; A segments: White; B segments: Bluish green. (For interpretation of the references to colour in this figure legend, the reader is referred to the web version of this article).

Fig. 7 presents the number of aggregates N (an aggregate contains more than two nanoparticles), the average number n of nanoparticles (both P_1 and P_2) in the aggregates, and the fraction of nanoparticles aggregated R_s as functions of a_{P2A} for $a_{P2P2} = 80$, $a_{P1P2} = 30$, $a_{AB} = 40$. For $a_{P1A} = 30$, as a_{P2A} increases, the number of aggregates first increases and then decreases (Fig. 7a, circle). This occurs because small clusters are first generated, and later, the small clusters aggregate into larger ones (Fig. 7b, circle). For $a_{P1A} = 70$, the number of aggregates is small and changes only slightly as a_{P2A} increases (Fig. 7a, square). The fraction of aggregated

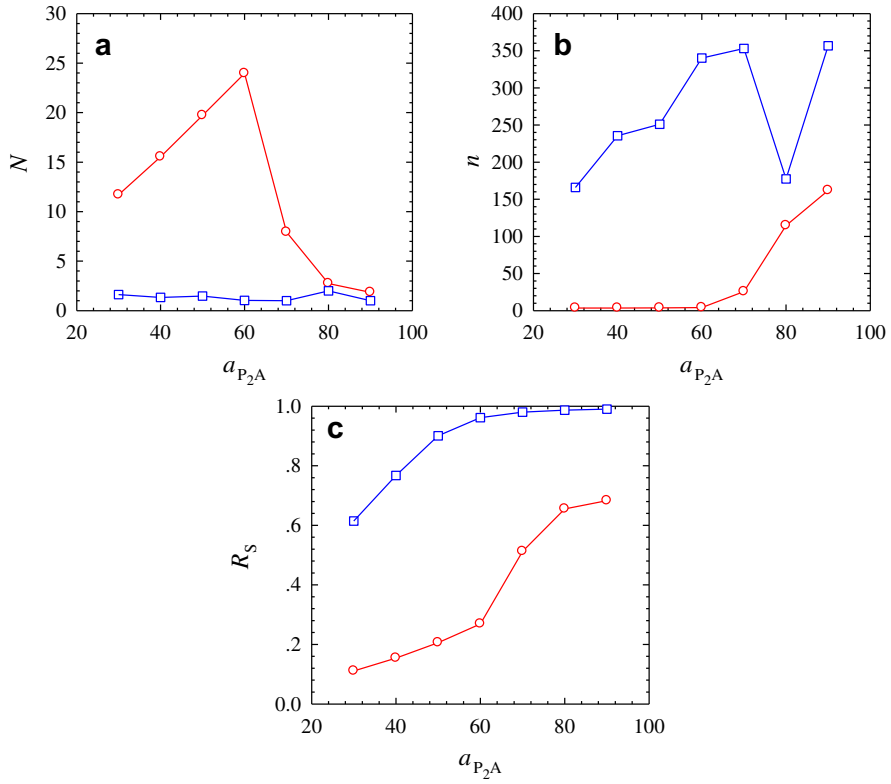

Fig. 7. Number of aggregates N (a), the average number n of nanoparticles (both P_1 and P_2) in aggregates (b), and the fraction of nanoparticles aggregated R_s (c), as functions of the pair repulsive interaction a_{P2A} between P_2 nanoparticles and A segments of the block copolymer A_5B_5 for $a_{P2P2} = 80$, $a_{P1P2} = 30$. Circle: $a_{P1A} = 30$; Square: $a_{P1A} = 70$.

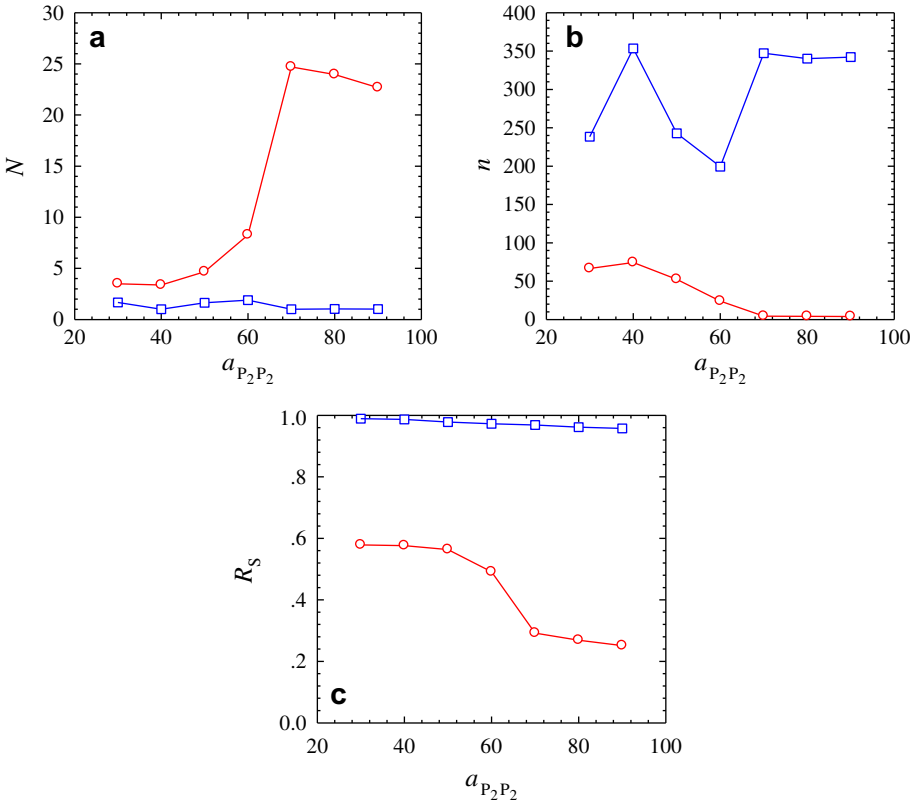

Fig. 8. Number of aggregates N (a), the average number n of nanoparticles (both P_1 and P_2) in aggregates (b), and the fraction of nanoparticles aggregated R_s (c), as functions of the repulsive pair interaction a_{P2P2} between P_2 nanoparticles for $a_{P2A} = 60$, $a_{P1P2} = 30$. Circle: $a_{P1A} = 30$; Square: $a_{P1A} = 70$.

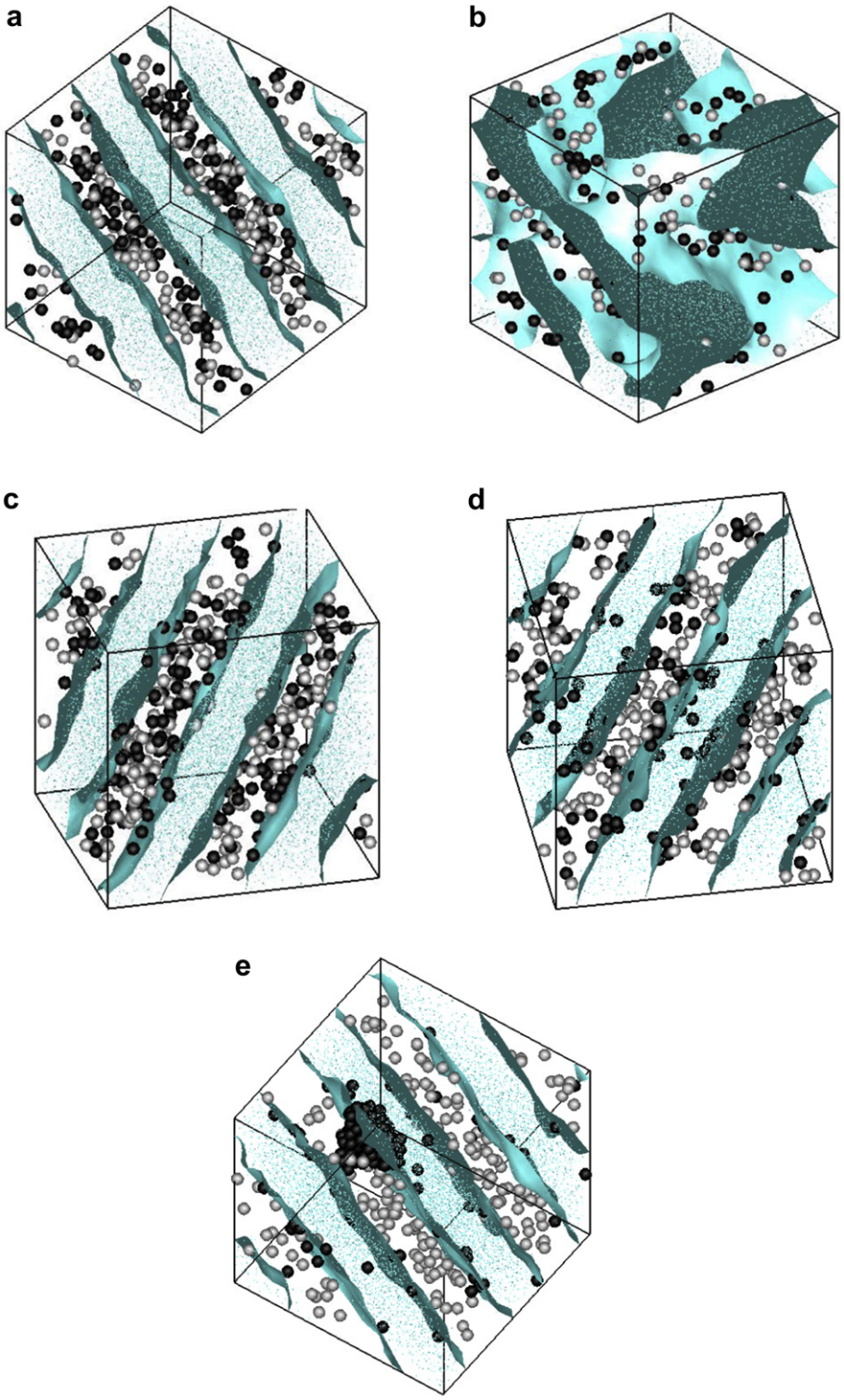

Fig. 9. Phase behavior of a binary mixture of nanoparticles-block copolymer composites as a function of the pair repulsive interaction a_{P2A} between P_2 nanoparticles and A segments of the block copolymer A_5B_5 for $a_{P1A} = 30$, $a_{P2P2} = 80$, $a_{P1P2} = 70$. (a) $a_{P2A} = 30$; (b) $a_{P2A} = 40$; (c) $a_{P2A} = 50$, 60; (d) $a_{P2A} = 70$; (e) $a_{P2A} = 80$, 90; P_1: Grey; P_2: Black; A segments: White; B segments: Bluish green. (For interpretation of the references to colour in this figure legend, the reader is referred to the web version of this article).

nanoparticles R_s increases as a_{P2A} increases (Fig. 7c). The values of R_s for $a_{P1A} = 70$ are always larger than those for $a_{P1A} = 30$ because the higher repulsion seems to stimulate the aggregation of the P_1 particles (see the explanation in Section 3.1). As a_{P2A} increases, a larger number of P_2 particles becomes aggregated.

The number of aggregates N, the average number n of nanoparticles (both P_1 and P_2) in the aggregates, and the fraction of nanoparticles aggregated R_s, are presented in Fig. 8 as functions of the repulsive pair interaction a_{P2P2} for $a_{P2A} = 60$, $a_{P1P2} = 30$, $a_{AB} = 40$. In Fig. 8a and b, a few large aggregates are generated for

$a_{P1A} = 30$ and a_{P2P2} smaller than 60. However, a sharp increase in the number of aggregates N and a sharp decrease in the average number of particles in the aggregates n occurs for a_{P2P2} larger than 60. This observation indicates the existence of a critical value of a_{P2P2} for aggregates to be generated when $a_{P1A} = 30$. For $a_{P1A} = 70$, a few large aggregates are generated (Fig. 8a and b, square) and almost all nanoparticles are aggregated. In contrast for $a_{P1A} = 30$, about 60% of the nanoparticles are aggregated for small values of a_{P2P2}, and small numbers of nanoparticles are aggregated for larger values of a_{P2P2}.

3.3. Phase behavior of a binary mixture of nanoparticles-block copolymer composites for strong a_{P1P2} interactions

Fig. 9 presents the phase behavior of a binary mixture of nanoparticles-block copolymer composites as a function of a_{P2A} for $a_{P1A} = 30$, $a_{P2P2} = 80$, $a_{P1P2} = 70$, $a_{AB} = 40$. Lamellae of the segments of the block copolymers are formed and both P_1 and P_2 particles are located for $a_{P2A} = 30$ in the A domains (Fig. 9a). As a_{P2A} increases to 40 (Fig. 9b), the lamellae are replaced by a complex structure. For $a_{P2A} = 50$ or 60, lamellae are again formed (Fig. 9c). Small clusters of P_1 and of P_2 are generated for $a_{P2A} = 70$. As a_{P2A} increases to 80 (Fig. 9d), the size of the clusters containing P_2 particles increases, and P_1 particles are located in the A domains whereas the P_2 particles prefer to be located at the interface between the A and B domains. These morphologies agree with the experimental data obtained by Bockstaller et al. [19]. For $a_{P2A} = 90$ (Fig. 9e), the P_2 aggregates are located at the interface between the A and B domains, whereas the nonaggregated P_1 particles are located in the A domain.

Fig. 10 presents the phase behavior of a binary mixture of nanoparticle-block copolymer composites as a function of the repulsive pair interaction a_{P2A} for $a_{P1A} = 70$, $a_{P2P2} = 80$, $a_{P1P2} = 70$. The strong repulsive pair interactions between the two kinds of nanoparticles, the strong repulsive pair interactions between the P_2 particles, and the weak repulsive interactions between the P_1 particles, generate the aggregation of P_1 (Fig. 10). By increasing a_{P2A}, the P_2 particles become increasingly aggregated. Some of

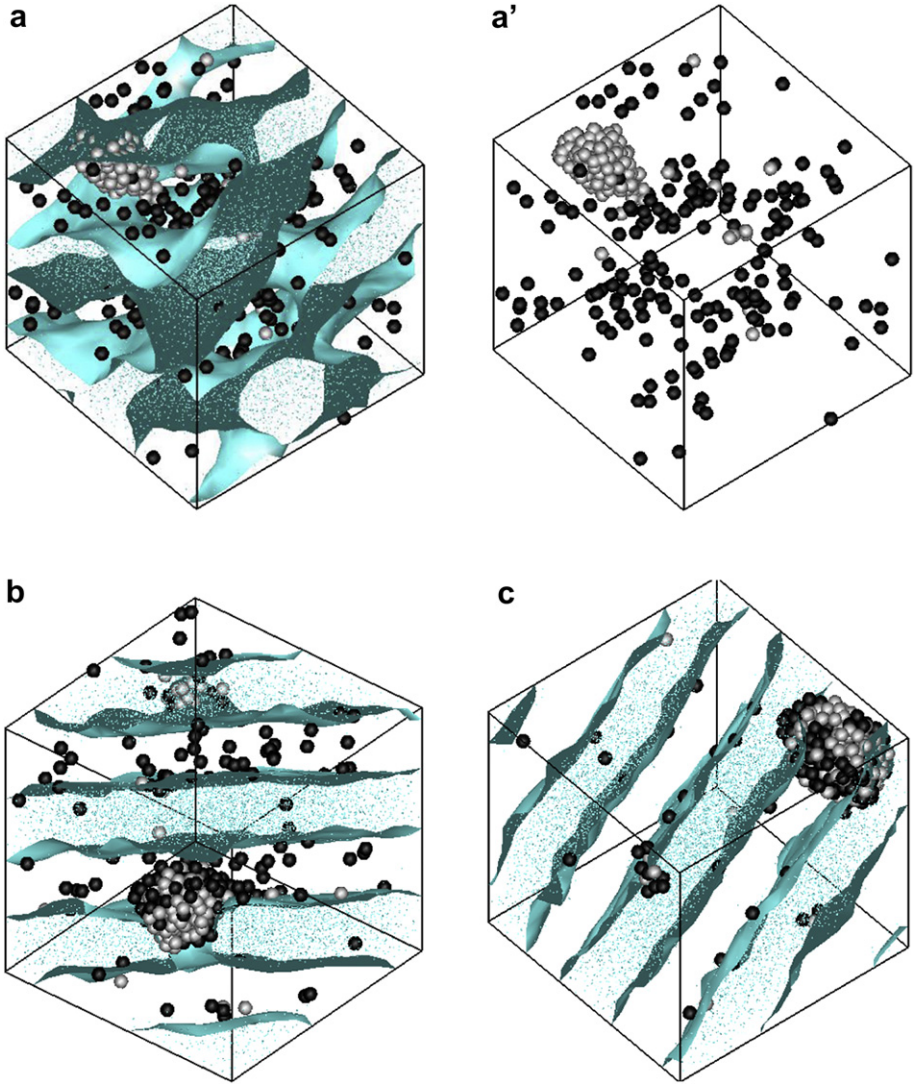

Fig. 10. Phase behavior of a binary mixture of nanoparticles-block copolymer composites as a function of the pair repulsive interaction a_{P2A} between P_2 nanoparticles and A segments of the block copolymer A_5B_5 for $a_{P1A} = 70$, $a_{P2P2} = 80$, $a_{P1P2} = 70$. (a) $a_{P2A} = 30$, 40; (b) $a_{P2A} = 50$, 60; (c) $a_{P2A} = 70$, 80, 90. P_1: Grey; P_2: Black; A segments: White; B segments: Bluish green. In Figure (a′), contains only the particles of Figure (a). (For interpretation of the references to colour in this figure legend, the reader is referred to the web version of this article).

the aggregates contain only P_2 particles, but other aggregates contain both kinds of particles. A large core-shell aggregate is generated (Fig. 10c) containing P_1 particles inside and P_2 particles outside. In addition, Fig. 10 shows that the aggregates are located at the interface between the A and B domains, whereas non-aggregated nanoparticles (mostly P_2) are located in the A domains.

Fig. 11 presents the phase behavior of a binary mixture of nanoparticles-block copolymer composites as a function of the repulsive interaction a_{P2P2} for $a_{P1A} = 30$, $a_{P2A} = 60$, $a_{P1P2} = 70$. For $a_{P2P2} = 30$ or 40, the P_2 particles aggregate and the block copolymer acquires a lamellar structure. Some lamellae are distorted by the presence of large aggregates (Fig. 11a). When a_{P2P2} increases to 50, a complex structure is formed (Fig. 11b). For a_{P2P2} from 60 to 80, lamellae are generated again, and the P_2 aggregates split into small clusters located at the interface between the A and B domains (Fig. 11c). For $a_{P2P2} = 90$, the two kinds of nanoparticles are distributed individually or as small clusters in the A domains (Fig. 11d).

Let us compare Figs. 6 and 11 with Figs. 4 and 9. In Figs. 6 and 11, the change of the state of the particles from aggregated to individually distributed is induced by the interactions between particles, and this changes the configuration of the block copolymer from lamellar to a complex one. In contrast, for the conditions selected for Figs. 4 and 9, the above change in the configuration of the particles (aggregated or nonaggregated) is induced by the interactions between the particles and the segments of the block copolymer, and does not affect the configuration of the block copolymer which remains lamellar.

Fig. 12 presents the number of aggregates N, the average total number n of nanoparticles (both P_1 and P_2) in the aggregates, and the fraction of nanoparticles aggregated R_s, as functions of the repulsive pair interaction a_{P2A} for $a_{P2P2} = 80$, $a_{P1P2} = 70$, $a_{AB} = 40$. For $a_{P1A} = 30$, as a_{P2A} increases, the number of aggregates N first increases and then decreases. The average number n of nanoparticles in the aggregates first changes slightly and then increases. This indicates that, as a_{P2A} increases, the number of clusters increases, whereas the size of these clusters changes slightly; further, the small clusters are replaced by larger ones. For $a_{P1A} = 70$, as a_{P2A} increases, the number of aggregates N changes slightly, while the size of the aggregates first changes a little, but further increases and contains both P_1 and P_2 particles.

Fig. 13 presents the number of aggregates N, the average number n of nanoparticles (both P_1 and P_2) in the aggregates, and the fraction of nanoparticles aggregated R_s, as functions of the pair repulsive interaction a_{P2P2} for $a_{P2A} = 60$, $a_{P1P2} = 70$, $a_{AB} = 40$. For small a_{P1A} ($a_{P1A} = 30$), as a_{P2P2} increases, aggregates are first generated; further, the aggregates split into numerous single nanoparticle or small clusters. This indicates the existence of a critical value of the interaction a_{P2P2} for aggregation to occur. For large a_{P1A} ($a_{P1A} = 70$), when a_{P2P2} changes between 30 and 90, large aggregates containing both P_1 and P_2 are generated. As a_{P2P2} further increases, some single nanoparticle P_2 separate from the aggregates, and the average number of particles in the aggregates decreases.

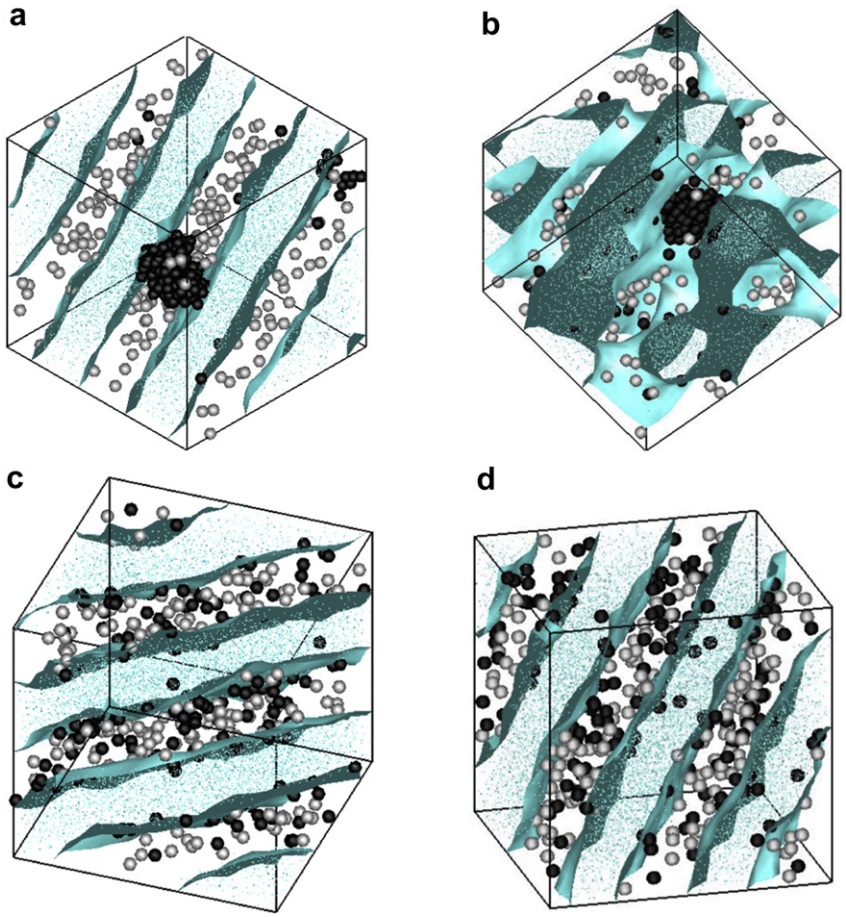

Fig. 11. Phase behavior of a binary mixture of nanoparticles-block copolymer composites as a function of the pair repulsive interaction a_{P2P2} between P_2 nanoparticles for $a_{P1A} = 30$, $a_{P2A} = 60$, $a_{P1P2} = 70$. (a) $a_{P2P2} = 30$, 40; (b) $a_{P2P2} = 50$; (c) $a_{P2P2} = 60$, 70, 80; (d) $a_{P2P2} = 90$. P_1: Grey; P_2: Black; A segments: White; B segments: Bluish green. (For interpretation of the references to colour in this figure legend, the reader is referred to the web version of this article).

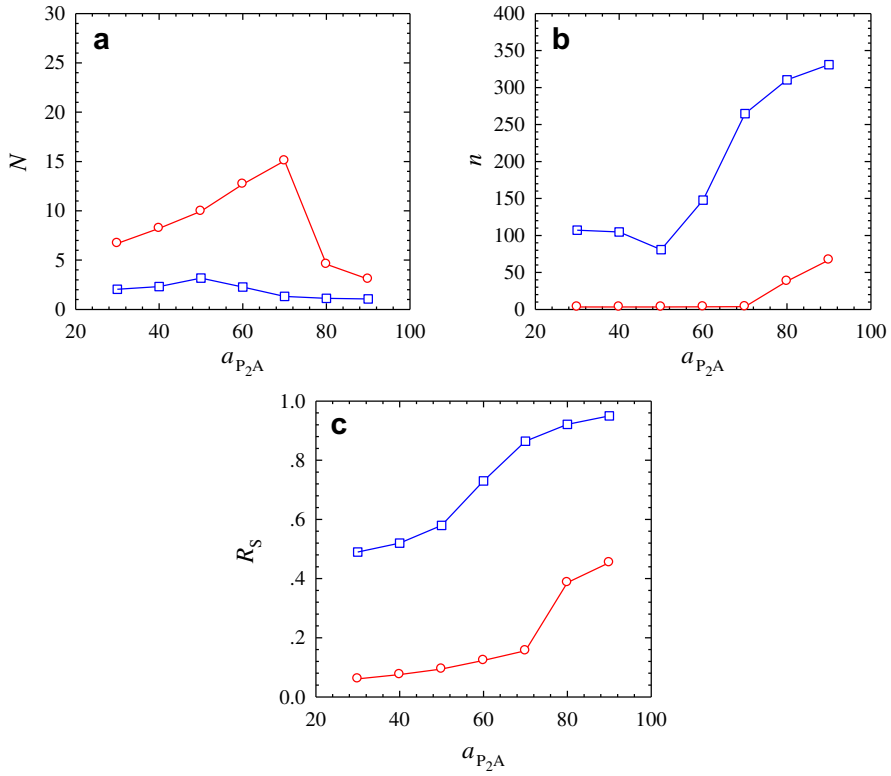

Fig. 12. Number of aggregates N (a), the average number n of nanoparticles (both P_1 and P_2) in aggregates (b), and the fraction of nanoparticles aggregated R_s (c), as functions of the pair repulsive interaction a_{P2A} between P_2 nanoparticles and A segments of the block copolymer A_5B_5 for $a_{P2P2} = 80$, $a_{P1P2} = 70$. Circle: $a_{P1A} = 30$; Square: $a_{P1A} = 70$.

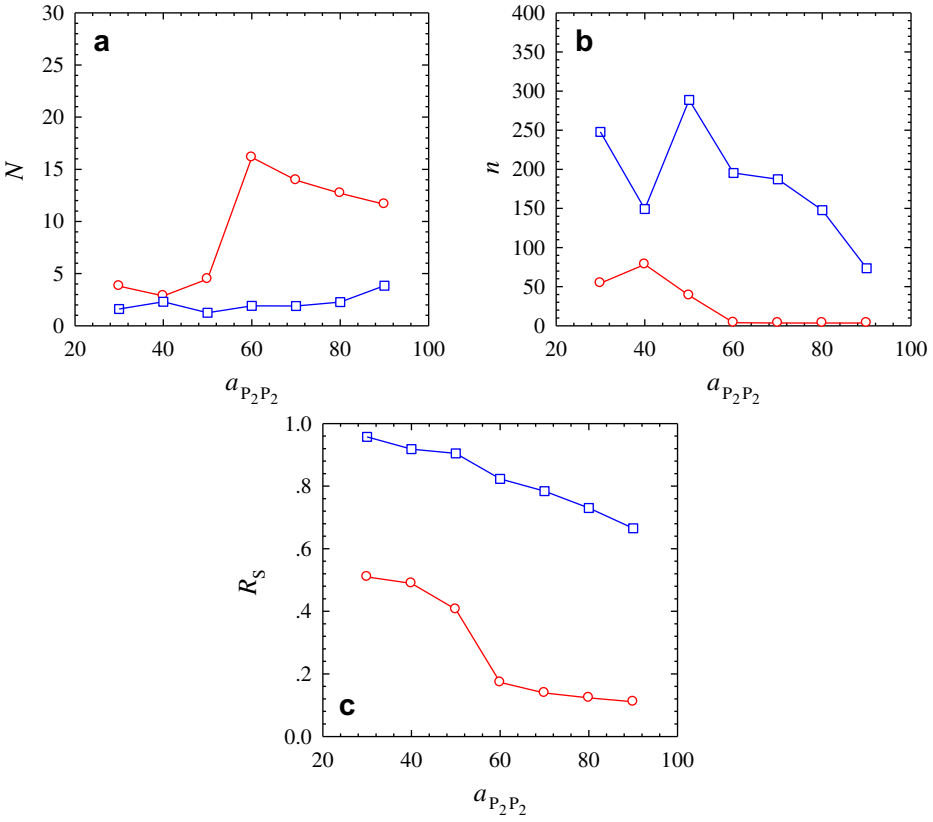

Fig. 13. Number of aggregates N (a), the average number n of nanoparticles (both P_1 and P_2) in aggregates (b), and the fraction of nanoparticles aggregated R_s (c), as functions of the pair repulsive interaction a_{P2P2} between P_2 nanoparticles for $a_{P2A} = 60$, $a_{P1P2} = 70$. Circle: $a_{P1A} = 30$; Square: $a_{P1A} = 70$.

3.4. Dynamic behavior of a binary mixture of nanoparticles-block copolymer composites

Figs. 14 and 15 present the dynamic behavior of a binary mixture of nanoparticles-block copolymer composites. The initial configuration was generated randomly (Fig. 14a). After 5000 steps (Fig. 14b), a fraction of particles aggregated as small clusters. A large aggregate, as well as a distorted lamellar structure of the block copolymer was found after 100 000 DPD steps (Fig. 14d). The P_1 and P_2 particles were located in the A domains. A perfect lamellar structure of the block copolymer and two aggregates are formed after 150 000 DPD steps (Fig. 14e). A very large aggregate was generated by the nanoparticles after 350 000 DPD steps(Fig. 14f). In Fig. 15, as the number of DPD steps increases, the number of

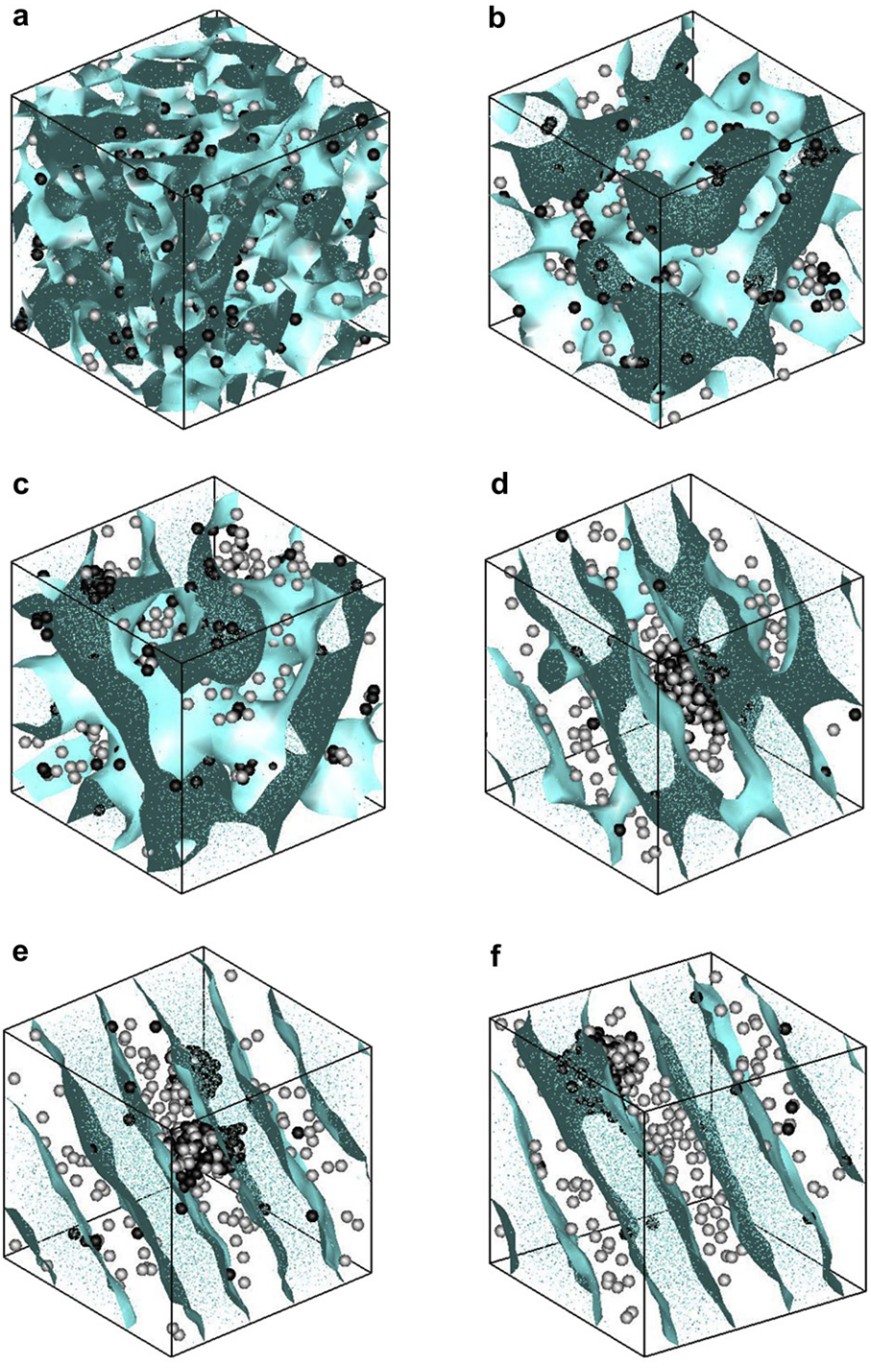

Fig. 14. Dynamics of aggregation of P_1 and P_2 nanoparticles blend and the evolution of block copolymer morphology for $a_{AA} = a_{BB} = 25$, $a_{AB} = 40$, $a_{P1P1} = 45$, $a_{P1B} = a_{P2B} = 80$, $a_{P1A} = 30$, $a_{P2P2} = 80$, $a_{P1P2} = 30$, $a_{P2A} = 90$. P_1: Grey; P_2: Black; A segments: White; B segments: Bluish green. (a) Initial; (b) after 5000 steps; (c) after 20 000 steps; (d) after 100 000 steps; (e) after 150 000 steps; (f) after 350 000 steps. Note: the initial configure of composite of this simulation was generated randomly. (For interpretation of the references to colour in this figure legend, the reader is referred to the web version of this article).

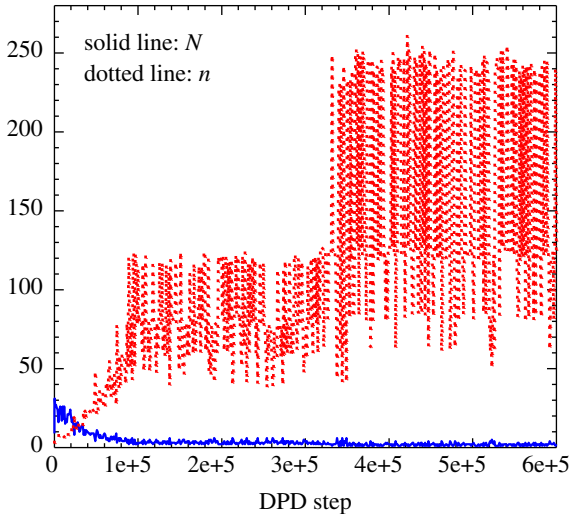

Fig. 15. Number of aggregates N, the average number n of nanoparticles (both P_1 and P_2) in aggregates as functions of DPD steps. Other conditions are the same as Fig. 14.

aggregates N first decreases sharply and then fluctuates steadily; the average number of nanoparticles in aggregates first increases, after which it fluctuates between 50 and 130 nanoparticles, and further fluctuates around a size between 70 and 240 nanoparticles.

4. Conclusions

By employing the dissipative particle dynamics (DPD) simulations, the morphology of a binary mixture of nanoparticles-block copolymer was examined by varying the pair interactions between the same and different kinds of nanoparticles, between the segments of the block copolymer, as well as the interactions between each kind of nanoparticles and each kind of segments of the block copolymer.

Even though the DPD considers only repulsive pair interactions, it is shown that compatibility can exist between the particles and the segments of the block copolymer and, as a result, various structures could be identified. For small values of a_{P1A} ($a_{P1A} = 30$), there is a critical interaction (a_{P2P2}) between the P_2 particles for them to become aggregated. However, for $a_{P1A} = 70$, no such critical value of a_{P2P2} exists. We found that the aggregates prefer to be located at the interface between the A and B domains, whereas single nanoparticle prefer to be located mostly in the A domains. Our findings indicate that, when the change of the state of the particles from aggregated to individually distributed is induced particularly by the interactions between particles, this changes the configuration of the block copolymer from lamellar to a complex one. In contrast, when the above change in the configuration of the particles (aggregated or nonaggregated) is induced particularly by the interactions between particles and segments of the block copolymer, it does not affect the configuration of the block copolymer which remains lamellar.

Acknowledgments

We wish to thank the Center for Computational Research in State University of New York at Buffalo for the computer time provided.

References

[1] Hamdoun B, Ausserre D, Joly S, Gallot Y, Cabuil V, Clinard C. J Phys II 1996;6:493.
[2] Hamdoun B, Ausserre D, Cabuil V, Joly S. J Phys II 1996;6:503.
[3] Lo C-T, Lee B, Pol VG, Dietz Rago NL, Seifert S, Winans RE, et al. Macromolecules 2007;40:8302.
[4] Bockstaller MR, Thomas EL. Phys Rev Lett 2004;93:166106.
[5] Chiu JJ, Kim BJ, Kramer EJ, Pine DJ. J Am Chem Soc 2005;127:5036.
[6] Kang H, Detcheverry FA, Mangham AN, Stoykovich MP, Daoulas KC, Hamers RJ, et al. Phys Rev Lett 2008;100:148303.
[7] Oh H, Green PF. Nat Mater 2009;8:139.
[8] Thompson RB, Ginzburg VV, Matsen MW, Balazs AC. Science 2001;292:2469.
[9] Thompson RB, Ginzburg VV, Matsen MW, Balazs AC. Macromolecules 2002; 35:1060.
[10] Wang Q, Nealey PF, de Pablo JJ. J Chem.Phys 2003;118:11278.
[11] Ginzburg VV, Qiu F, Balazs AC. Polymer 2002;43:461.
[12] Schultz AJ, Hall CK, Genzer J. Macromolecules 2005;38:3007.
[13] Huh J, Ginzburg VV, Balazs AC. Macromolecules 2000;33:8085.
[14] Kalra V, Mendez S, Escobedo F, Joo YL. J Chem Phys 2008;128:164909.
[15] Huang J, Sun D. J Colloid Interf Sci 2007;315:355.
[16] Jin J, Wu J. J Chem Phys 2008;128. 074901.
[17] Matsen MW, Thompson RB. Macromolecules 2008;41:1853.
[18] Chen H, Ruckenstein E. J Chem Phys 2009;131:244904.
[19] Bockstaller MR, Lapetnikov Y, Margel S, Thomas EL. J Am Chem Soc 2003; 125:5276.
[20] Espanol P, Warren P. Europhysics Lett 1995;30:191.
[21] Feng J, Liu HL, Hu Y. Macromol Theory Simulat 2006;15:674.
[22] Huang JH, Wang YM. J.Phys Chem B 2007;111:7735.
[23] Lisal M, Brennan JK. Langmuir 2007;23:4809.
[24] Groot RD, Madden TJ. J Chem Phys 1998;108:8713.
[25] Groot RD. Langmuir 2000;16:7493.
[26] Hoogerbrugge PJ, Koelman J. Europhysics Lett 1992;19:155.
[27] Groot RD, Warren PB. J Chem Phys 1997;107:4423.
[28] (a) Liu DH, Zhong CL. Macromol Rapid Communicat 2006;27:458;
(b) He L, Zhang L, Liang H. Polymer 2010;51:3303.